APTECH IS APPLIED TECHNOLOGY ®

AES 90051243-1Q-1
Revision 1

QA Record

B26 '90 0627 301

ANALYSIS OF HVAC DUCTS IN TENNESSEE VALLEY AUTHORITY'S WATTS BAR NUCLEAR PLANT, UNITS 1 AND 2

Prepared by

Geoffrey R. Egan
Philip M. Besuner
Marvin J. Cohn
Steve R. Paterson

Aptech Engineering Services, Inc.
1257 Elko Drive
Sunnyvale, California 94089

Prepared for

Tennessee Valley Authority
Watts Bar Nuclear Plant
Post Office Box 800
Spring City, Tennessee 37381

Attention: Mr. Roger Alley

June 1990

9007120348 900629
PDR ADOCK 05000390
S PDC

ENCLOSURE 1

PLAN FOR FUNCTIONAL TESTING OF HEATING, VENTILATING, AND AIR CONDITIONING (HVAC) DUCT

Functional and leak tests were performed as part of the original startup program on systems with welded ductwork. As part of the current prestart test program, the following systems will be functionally retested and documented in accordance with the test scoping documents.

DOCUMENT	SYSTEM
TVA-1	Emergency Gas Treatment System (EGTS)
TVA-9	Auxiliary Building Gas Treatment System (ABGTS) and Reactor Building Purge System NOTE: Includes the portion of the post accident sampling which is required for ABGTS pressure boundary
TVA-10	Control Building Heating Ventilating and Air Conditioning Systems
TVA-6	Containment Air Return System (CARS) (Hydrogen Collection System)
TVA-14C	Diesel Generator Battery Hood Exhaust

The Watts Bar restructured standard Technical Specification submitted to NRC requires surveillance testing of the ABGTS and EGTS. These surveillance tests will verify that system flow rates can be obtained indicating that the ductwork is functional.

ENCLOSURE 2

APTECH EVALUATION REPORT

TENNESSEE VALLEY AUTHORITY
WATTS BAR NUCLEAR PLANT

Structural Integrity Evaluation of HVAC Duct
Weldments at Watts Bar Nuclear Plant

VERIFICATION RECORD SHEET REPORT NO.: AES 90041243-1Q-1

Originated by _____ 6-25-90
Geoffrey R. Egan, Project Manager — Date
Aptech Engineering Services, Inc.

Verified by _____ 6/25/90
Russell C. Cipolla, Verifier — Date
Aptech Engineering Services, Inc.

Quality Assurance _____ 25 JUN 90
Jeffrey L. Grover, Quality Assurance Engineer — Date
Aptech Engineering Services, Inc.

Quality Assurance _____ 25 JUN 90
Jeffrey L. Grover, Acting Quality Assurance Manager — Date
Aptech Engineering Services, Inc.

TABLE OF CONTENTS

Section		Page
	SUMMARY AND CONCLUSIONS	iii
1	INTRODUCTION AND OBJECTIVE	1-1
	Objective	1-2
	Scope	1-2
	References	1-2
2	ANALYSIS METHODS	2-1
	Fracture Mechanics Background	2-1
	Limit Load Analysis	2-2
	References	2-3
3	ANALYSIS OF STRESSES	3-1
	References	3-2
4	CHARACTERIZATION OF MATERIAL PROPERTIES	4-1
	Introduction	4-1
	Strength Properties	4-1
	Fatigue Crack Growth Rates	4-2
	References	4-3
5	COMPARISON OF DESTRUCTIVE TEST RESULTS WITH LIMIT LOAD PREDICTIONS	5-1
	Introduction	5-1
	Limit Load Analysis Predictions	5-2
	References	5-4
6	WORST CASE FLAW SIZES AND APPARENT STRENGTH	6-1
	Introduction	6-1
	Formulation of the Statistics Problem	6-2
	Assumptions	6-2
	Results	6-3
	References	6-3
7	FITNESS-FOR-SERVICE EVALUATION	7-1
	Introduction	7-1
	Evaluation of Subcritical Crack Growth	7-1
	Limit Load Evaluation	7-2
	Results	7-2
	Conservatisms in the Analysis	7-2
	References	7-3

Section		Page
8	CONCLUSIONS	8-1
	APPENDIX A - STATISTICAL ANALYSIS METHOD	A-1

SUMMARY AND CONCLUSIONS

This report describes the methods and results of a structural integrity analysis to evaluate the fitness for service of the heating, ventilating, and air conditioning (HVAC) ductwork at the Watts Bar Nuclear Plant, Units 1 and 2.

The weld imperfections analyzed include lack of penetration and sections of weld missing in the duct-to-duct butt welds.

Stress analysis data have been reviewed to establish the highest stresses for any load combination including design basis accidents. These stresses have been used to calculate the limiting imperfection sizes for failure by plastic collapse.

In addition, field inspection have been used to establish worst case flaw sizes based on the statistical 95% probability of occurrence and the 95% confidence level. These "95-95" data have been compared with the limit flaw sizes determined from the analyses method.

Destructive tests have also been performed to establish the strength of welds containing weld flaws. Test data were also used to confirm that the analysis method was accurate and conservative.

It was concluded that:

- Limit load analysis methods conservatively predicted the failure conditions for HVAC ductwork containing potential weld flaws.
- Test results on samples removed from the ductwork confirmed the analysis methods and the strength of the welds.
- Inspection data have been used to establish statistical worst case values for the two weld attributes considered. The results for a "95-95" worst case are 53% for lack of penetration and 17% for potential "missing" weld.

- Even with these conservative worst case estimates of weld attributes, significant margins against failure are shown to exist when analyzed using a method based on ASME Boiler and Pressure Vessel Code, Section XI and worst case stresses for operating basis earthquake (OBE) and safe shutdown earthquake (SSE).

The analysis results, the field inspections, and the test data confirm that the HVAC ductwork is suitable for the design loads for which it was intended.

Section 1
INTRODUCTION AND OBJECTIVE

Concerns regarding the quality and technical requirements for the early constructed HVAC ducts at Watts Bar Nuclear Plant have led to a program to evaluate the significance of weld imperfections in some of the welds in the ductwork. Specifically duct-to-duct welds may contain lack of penetration. Further, although all ductwork has passed the leak test requirements there were some regions examined in which there were sections of weld missing.

Review and inspection programs by Tennessee Valley Authority (TVA) have identified the scope of this problem. The current work addresses the significance of weld imperfections in the following duct types:

- Spiral welded round duct (e.g., ASTM A211, eight-inch diameter to 36-inch diameter, 14 gauge to 0.134-inch wall thickness)
- Rectangular ducts (e.g., 24-inch to 28-inch x 96-inch, 12-gauge (0.1046 inch) wall thickness)
- Scheduled pipe (e.g., ASTM A106, Grade B, six-inch to 24-inch diameter, 1/4-inch to 5/16-inch wall thickness)

All the circumferential welds were fabricated with Type E7018 weld metal. The concern in each case is that the weld imperfections may, if unrepaired, lead to early structural failure. This report addresses that concern and does so by evaluating the potential for defect growth by a fatigue mechanism and concurrent or subsequent failure by ductile plastic collapse.

This report presents the methods used and the analysis results to update the preliminary analyses reported earlier (1-1).

Three specific refinements are included in this report that differ from the preliminary analysis as follows:

- The limiting stress is for the postaccident sampling system and for the normal/upset condition is 8.93 ksi which consists mainly of an 8.45 ksi contribution from thermal expansion (Section 3, Table 3-2).
- The "worst case" missing weld data have been reviewed and an upper bound established at 17% (Section 6).
- Fatigue crack growth, which is shown to be negligible, has also been considered.

OBJECTIVE

The specific objective of this program was to develop a structural integrity analysis to assure that the HVAC ductwork welds would perform their intended function.

SCOPE

The remainder of this report consists of seven sections. Section 2 outlines the analysis methods that have been used to evaluate the imperfections. The next four sections introduce and discuss input to the analytical model. These sections include: evaluation of applied stresses (Section 3), characterization of material properties (Sections 4 and 5), and establishment of statistically based worst case weld attributes (Section 6). The information in Sections 2 through 6 form the basis of the fitness-for-service evaluation in Section 7. Conclusions drawn from these evaluations are listed in Section 8.

REFERENCES

1-1 "Safety-Related Heating Ventilating and Air Conducting Duct Welding, Watts Bar Nuclear Plant", Meeting with NRC staff, Rockville, Maryland, May 31, 1990, Presentation Viewgraphs.

Section 2
ANALYSIS METHODS

The following sections discuss those aspects of fracture mechanics and fatigue theory which were used in the analysis of the present problem. A presentation of general fracture mechanics background is followed by a discussion of the specific methods of analysis to be used in this report.

FRACTURE MECHANICS BACKGROUND

The failure behavior of structures under monotonic (slowly increasing) loading can be classified into three regimes in which a specific type of failure mode is appropriate. These three regimes cover brittle fracture, ductile fracture and plastic collapse. The disciplines required to assess these regimes are:

- Linear elastic fracture mechanics (LEFM) - The structure fails in a brittle manner and, on a macro scale, the load to failure occurs within nominally elastic loading.
- Elastic-plastic fracture mechanics (EPFM) - The structure fails in a ductile manner, and significant stable crack extension by tearing may precede ultimate failure.
- Fully plastic instability (limit load theory) - The failure event is characterized by large deflections and plastic strains associated with ultimate strength collapse.

A diagram that shows the relationship between critical or failure stress and flaw size for the three failure modes is given in Figure 2-1. The shape and position of the failure locus will depend on the fracture toughness (K_{Ic}) and strength properties (σ_f) of the material, as well as the structural geometry and type of loading.

In the case of thin ductwork steel sections operating at or near room temperature failure under monotonic loading will occur by plastic collapse and the appropriate analyses method is limit

load. This is confirmed by a fractographic analysis of fracture surfaces of test samples pulled in tension as part of this program. These results are discussed in detail in Section 7.

Limit Load Analysis

For limit load analysis, the critical stress to cause failure is calculated from the net section plastic collapse relationship for circular pipe. The method used for this project is embodied in ASME Boiler and Pressure Vessel Code Case N-463 (2-1). The limit load is determined from the geometry of the section and the material properties as presented in the code case. After accounting for the reduction in area due to the flaw, the limit load can be expressed in terms of a limit stress and the geometric variables. The analyses have been performed using the assumption that the limit load conditions for all sections are approximated by the circular section calculations. In view of the implicit margins included in the analysis (Section 7), this is a reasonable assumption.

The limit stress or flow stress is the material yield strength when the material behavior is assumed to be elastic-perfectly-plastic. However, for materials which exhibit significant strain hardening, σ_f, could be somewhere between yield and ultimate strength, and the appropriate value to use should be determined by tests. For this analysis, we use a flow stress value, which is the average of the yield and ultimate strengths, i.e.:

$$\sigma_f = (\sigma_y + \sigma_{uts})/2 \qquad (2\text{-}1)$$

where σ_f is the flow stress, σ_y the specified minimum yield stress and σ_{uts} the specified minimum ultimate strength.

Once the limit conditions have been calculated, the expressions for applied membrane stress as a function of pressure and applied moment can be used to determine the failure condition.

As noted earlier and discussed in Section 7, for the thin section ducts addressed in this report, limit load failure is the expected controlling failure mode. The inputs required to model this failure mode are stresses, material properties, and flaw dimensions.

REFERENCES

2-1 American Society of Mechanical Engineers, "Cases of ASME Boiler Vessel Code, Case N-463, Evaluation Procedures and Acceptance Criteria For Flaws in Class 1 Ferritic Piping That Exceed the Acceptance Standards of IWB-3514.2, Section XI, Division 1" (Approval Date: November 30, 1988).

APTECH®
ENGINEERING SERVICES, INC.
© 1990 APTECH

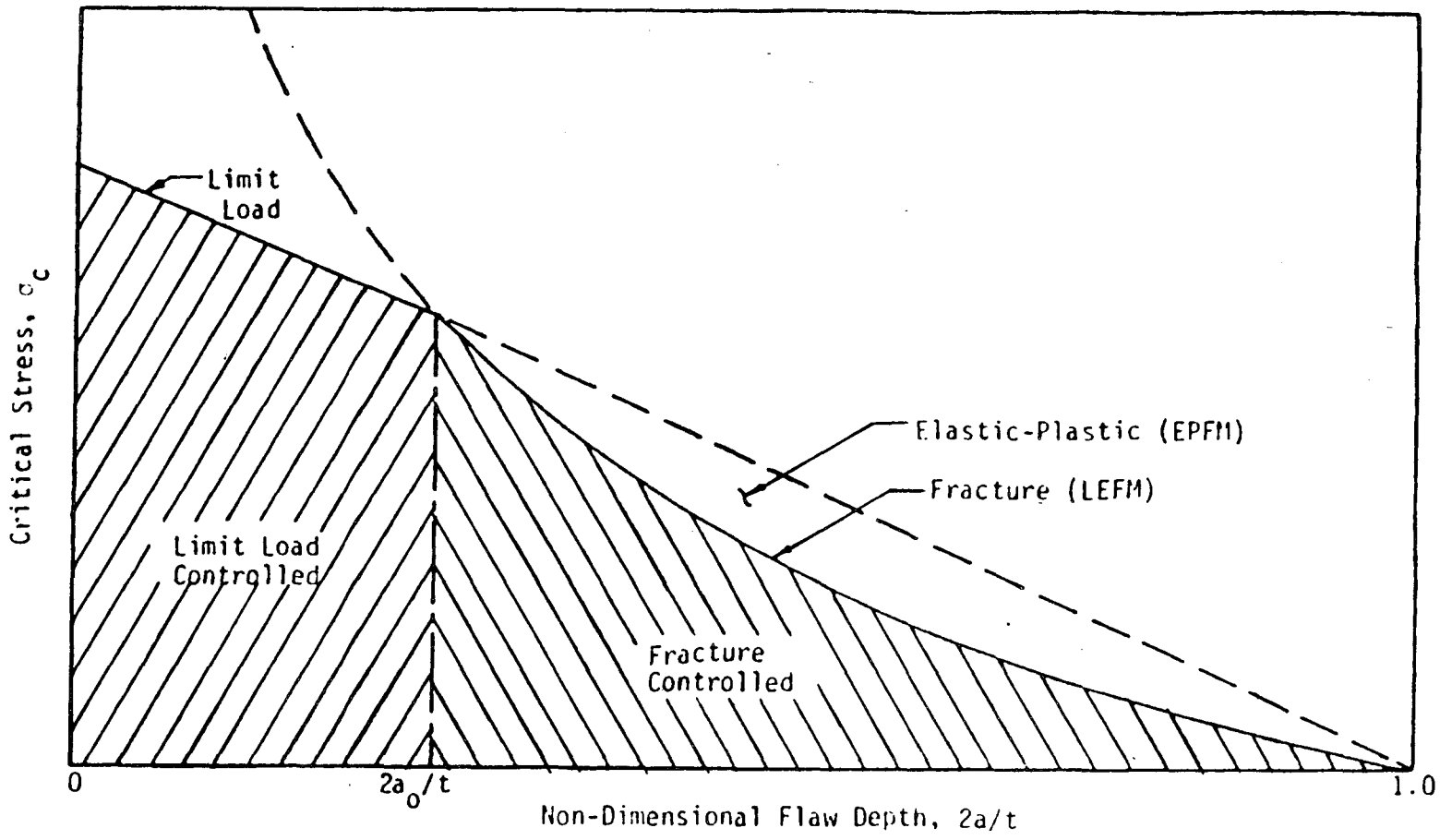

Figure 2-1 - Schematic Showing the Relationship Between Failure Stress and Flaw Size For Two Limiting Failure Modes.

Section 3
ANALYSIS OF STRESSES

The analytical model discussed in Section 2 used applicable stresses for any HVAC duct section. This section summarizes results of the stress analysis performed for the original HVAC ductwork (3-1) and pipe (3-2).

The most highly stressed joint and load combination was selected for each specified duct/pipe system. These bounding cases were used to assess any weld imperfection to assure a conservative analysis.

A review of the stress analysis data was performed to establish peak stresses for the expected plant loading conditions (3-3). A summary for the higher stressed HVAC sections is provided in Tables 3-1 and 3-2. Axial membrane, bending and shear stresses are tabulated.

The plastic collapse evaluation is based on the most severe load combinations determined for the HVAC ducts/pipes. Loads from the operating basis earthquake (OBE), safe shutdown earthquake (SSE) and applicable thermal displacements were evaluated for the worst case load combination. These worst case load combinations for the postulated events were used in the Section 7 bounding plastic collapse evaluations.

Some of the loading events are present during normal operation while others are anticipated to act only a few times over the life of the plant. High cycle fatigue is not considered a degradation mode because the high cycle stresses are of negligible magnitudes. A bounding fatigue analysis of the low cycle cyclic loads was performed to assess the potential for promoting subcritical flaw growth.

REFERENCES

3-1 Tennessee Valley Authority, "HVAC Ductwork - Evaluations For Safety Significance of Duct Welding Concerns", WCG-1-500, Rev. 2, RIMS B269001618151 (June 16, 1990).

3-2 Tennessee Valley Authority, "Assessment of Structural Integrity of HVAC Welds", QIR CEB-WBN-90-638, RIMS B26900612121 (June 12, 1990).

3-3 Aptech Engineering Services, Inc., "Review of HVAC Stress Analyses Applied to Welds", APTECH Project AES 90051243, Calculation 1 (June 25, 1990), Revision 2.

APTECH
ENGINEERING SERVICES, INC
© 1990 APTECH

Table 3-1

HVAC DUCT STRESS SUMMARY

Component	Stresses (ksi) Membrane	Bending	Shear
P + DW + SSE (Faulted) Load Combination			
Spiral welded round duct	0.02	7.66	1.82
EGTS 24" diameter duct (Areas 1 to 6)	0.87	2.48	1.25
EGTS 24" x 24" duct (Areas 1 to 6)	2.90	3.23	0.98
EGTS 14" diameter duct (Areas 7, 9, and 10)	0.02	8.37	1.8
EGTS 24" x 24" (Area 8)	2.23	3.11	1.08
EGTS Areas 11 through 16	6.87	2.09	1.28
Containment purge air	0.02	1.21	---
14" diameter duct	0.02	9.67	---
Pant leg 60" x 36" to 2 - 36" x 36"	5.59	1.13	---
Original analysis for the faulted load combination (Ref. (1-1))	4.88	4.88	---
P + DW + OBE (Upset) Load Combination			
Spiral welded round duct	0.02	3.92	0.93
EGTS 24" diameter duct	0.83	2.36	1.20
EGTS 24" x 24" duct (Areas 1 to 6)	2.76	2.61	0.94
EGTS 24" x 24" duct (Area 8)	2.23	1.70	1.03
EGTS 14" diameter to 16" x 16" intersection	6.87	0.00	0.75
Original analysis for the upset load combination (Ref. (1-1))	3.63	3.63	---

Table 3-2

HVAC PIPE STRESS SUMMARY

System	Loading Condition	Bending Stress[1] (ksi)
Postaccident sampling[2]	Secondary[6]	8.45
Postaccident sampling	Upset[4]	0.48
Postaccident sampling	Faulted[5]	0.75
Hydrogen collection[3]	Secondary[6]	2.97
Hydrogen collection	Upset[4]	3.28
Hydrogen collection	Faulted[5]	5.66

[1]Membrane and shear stresses are negligible.
[2]12.759-inch diameter pipe, 0.375-inch wall thickness
[3]8.625-inch diameter pipe, 0.322-inch wall thickness
[4]From Code Equation 9U
[5]From Code Equation 9F
[6]From Code Equation 11

Section 4
CHARACTERIZATION OF MATERIAL PROPERTIES

INTRODUCTION

This section documents the basis for the material properties used in the limit load analyses in Section 5 and the fitness-for-service evaluation in Section 7. The material properties which will determine the flaw tolerance of these thin section duct weldments are the yield and ultimate strength values (used in the limit load assessment) and the fatigue crack growth rates.

STRENGTH PROPERTIES

The ultimate failure of the duct weldments will be determined by the limit or flow stress, σ_f, of the material. As described in Section 2, the flow stress is the average of the yield and ultimate strength of the material:

$$\sigma_f = (\sigma_y + \sigma_{uts})/2 \qquad (4\text{-}1)$$

where σ_f = flow stress, σ_y the minimum yield stress, and σ_{uts} the minimum ultimate tensile strength.

The flow stress used in the bounding limit load analyses presented in Section 7 was based on the specified minimum yield stress (25 ksi) and ultimate strength (45 ksi) of ASTM A570 material. The flow stress in this case is 35 ksi.

A comparison of the ultimate strengths of destructively tested sections of duct welds (which included lack-of-penetration flaws) with limit load calculations made for the test geometry in Section 5 indicate that the flow stress of these weldments is significantly higher than 35 ksi. It is further shown (Section 5) that the flow strength of Type E7018 weld metal (70 ksi)

adequately predicts the failure conditions of these flawed weldments. The use of the flow stress for ASTM A570 Grade A (which is 1/2 the value of the flow stress of Type 7018 weld metal) provides a high safety margin on the strength of these weldments. Additional safety factors above and beyond this inherent weld metal strength margin were used in the fitness-for-service analyses in Section 7.

FATIGUE CRACK GROWTH RATES

In order to estimate the extent of crack growth that could occur over the design life of the plant, a fatigue evaluation was performed. This evaluation combined the cyclic stresses (Section 3) with the appropriate crack propagation rates (Section 4) to obtain the expected crack growth (Section 7).

The purpose of this section is to assess propagation rates for flaw growth by a fatigue mechanism. Because the cracks are located in the weldments, this requires an evaluation of carbon steel weld metal crack growth data. References have been drawn together to estimate a conservative bound on potential crack growth rate. A conservative bound implies the fastest possible rate of crack growth. Several data sets are available for the E7018 weld metal in the as-welded condition and these have been used to estimate bounding values of crack growth rate.

The following engineering unit conventions are in effect unless otherwise stated:

- ΔK (stress intensity factor range), ksi $\sqrt{in}$
- T (temperature), °F
- da/dN (crack growth rate), inches/cycle

Data available in the literature were collected for all types of carbon steel weld metal with an emphasis on Type E7018. A study by Maddox (4-1), resulted in a substantial amount of crack growth data for four different weld metals including Type E7018. The crack growth data from Maddox are plotted in Figure 4-1. Crack growth data for the Type E7018 weld

material (Weld Metal C) are shown separately in Figure 4-2. Also shown on Figure 4-1 is the bounding line from similar testing on plain (unwelded) steels performed by Gurney (4-2).

Other data from similar weld metals (4-3) with and without stress relief, fall within the upper bound shown in Figure 4-1 for Gurney (4-2). The literature also states that weld metals for joining steels such as ASTM A516 Grade 70 exhibit slower fatigue growth rates than the base metals (4-4).

Residual stresses may increase crack growth rate (da/dN), but if these stresses are included in estimating crack growth rates, the data indicate that the bounding line by Gurney (4-2) will conservatively predict crack growth for Type E7018 weldments. Figure 4-3 shows the line which is represented by:

$$da/dN = 2.63 \times 10^{-10} \Delta K^{3.44} \qquad (4\text{-}2)$$

These data have been used to conservatively estimate the amount of crack growth expected in the plant from OBE or SSE cycling.

REFERENCES

4-1 Maddox, S. J., "Fatigue Crack Propagation in Weld Metal and Heat Affected Zone Material," The Welding Institute, Report No. E/29/69, Abington, Great Britain (1969).

4-2 Gurney, T. R., and S. J. Maddox, "A Reanalysis of Fatigue Data for Welded Joints in Steel," The Welding Institute, Welding Research International, Vol. 3, No. 4 (1973).

4-3 Seeley, R. R., L. Katz, and J. R. M. Smith, "Fatigue Crack Growth in Low Alloy Steel Submerged Arc Welds," Fatigue Testing of Weldments, Pp. 261 to 284.

4-4 Gurney, T. R., "An Investigation of the Rate of Propagation of Fatigue Cracks in a Range of Steels," The Welding Institute Members' Report No. E18/12/68.

APTECH
ENGINEERING SERVICES, INC
© 1990 APTECH

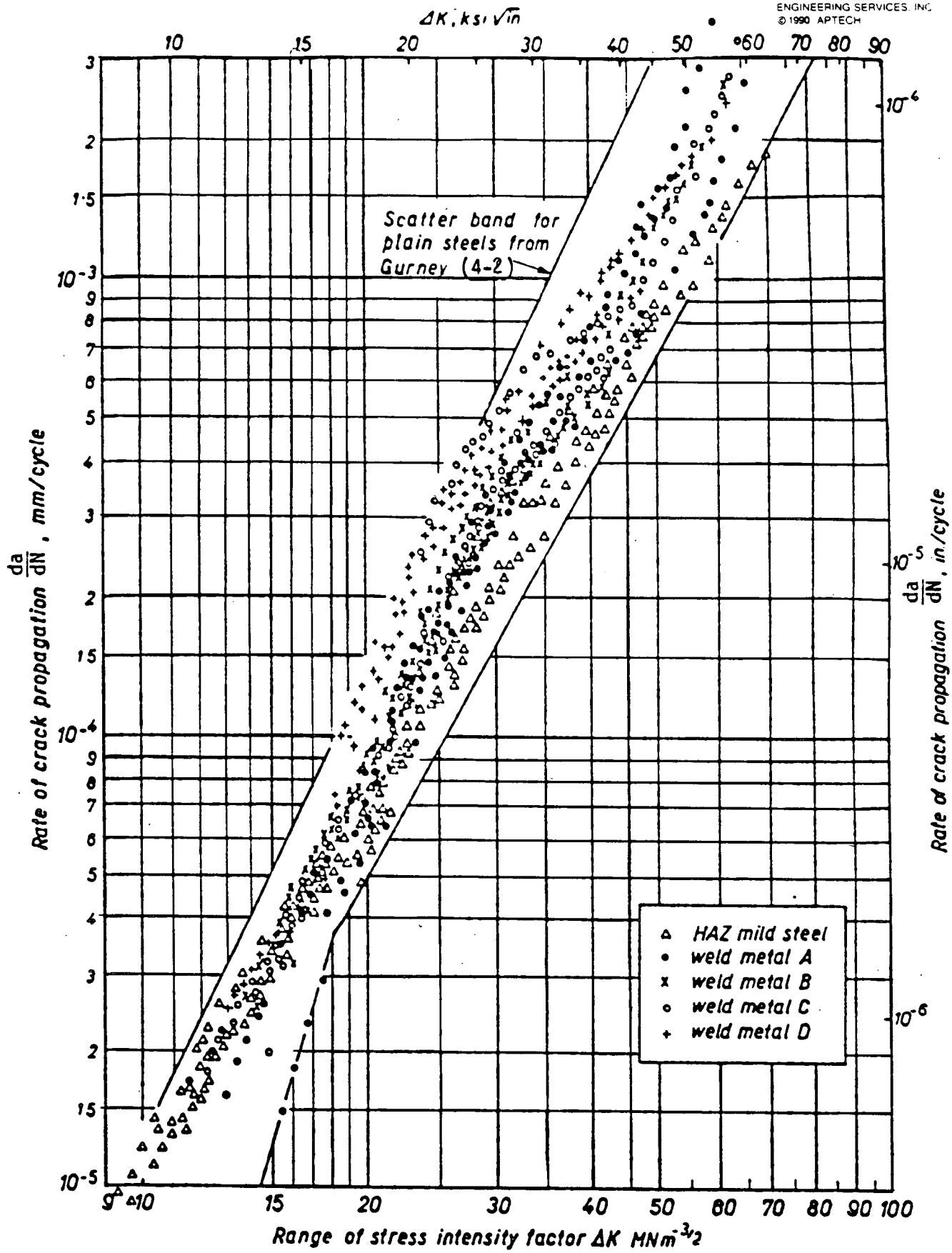

Figure 4-1 - Crack Growth Data From Maddox (4-1).

APTECH
ENGINEERING SERVICES, INC
© 1990 APTECH

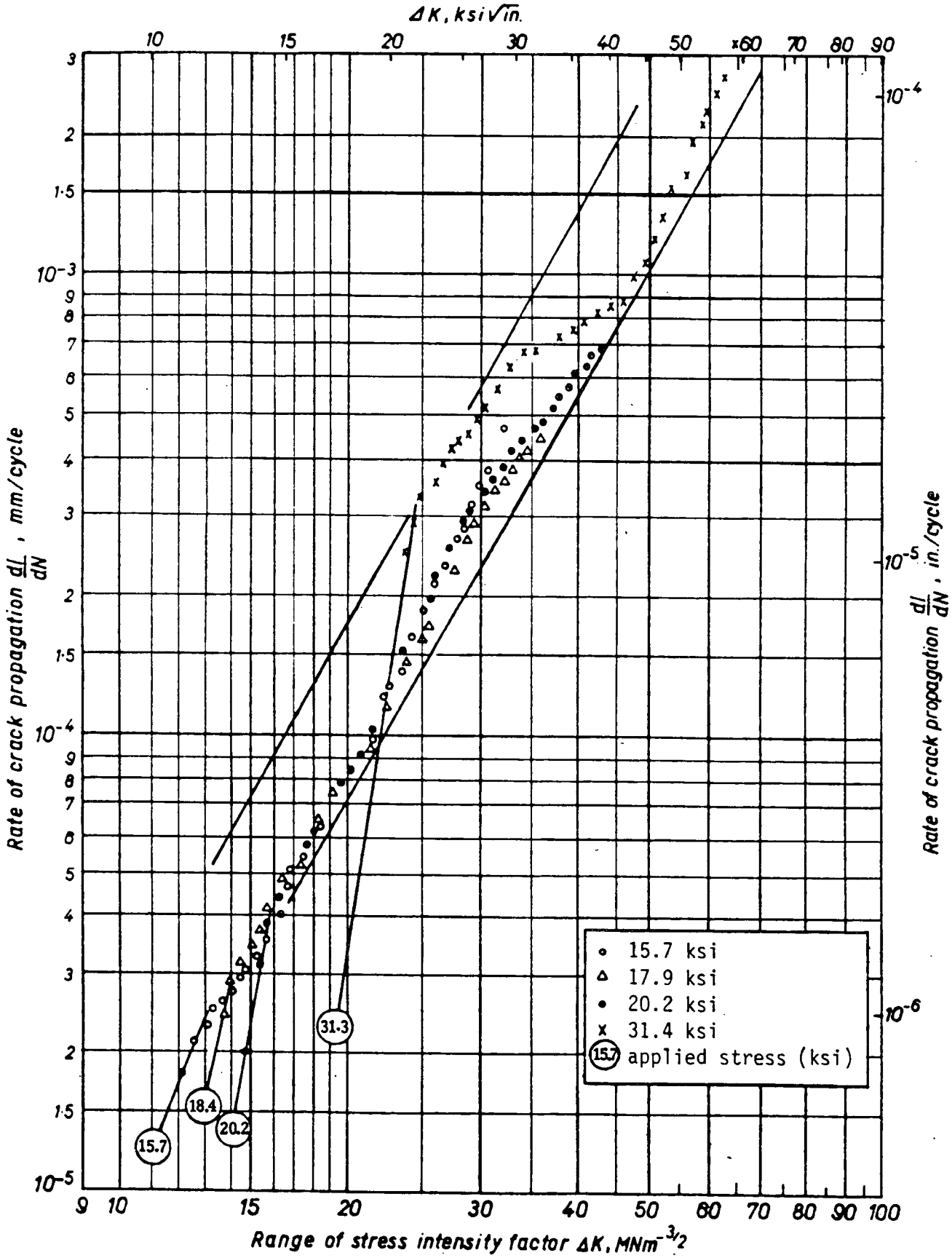

Figure 4-2 - Crack Growth Data For E7018 From Maddox (4-1).

APTECH
ENGINEERING SERVICES, INC
© 1990 APTECH

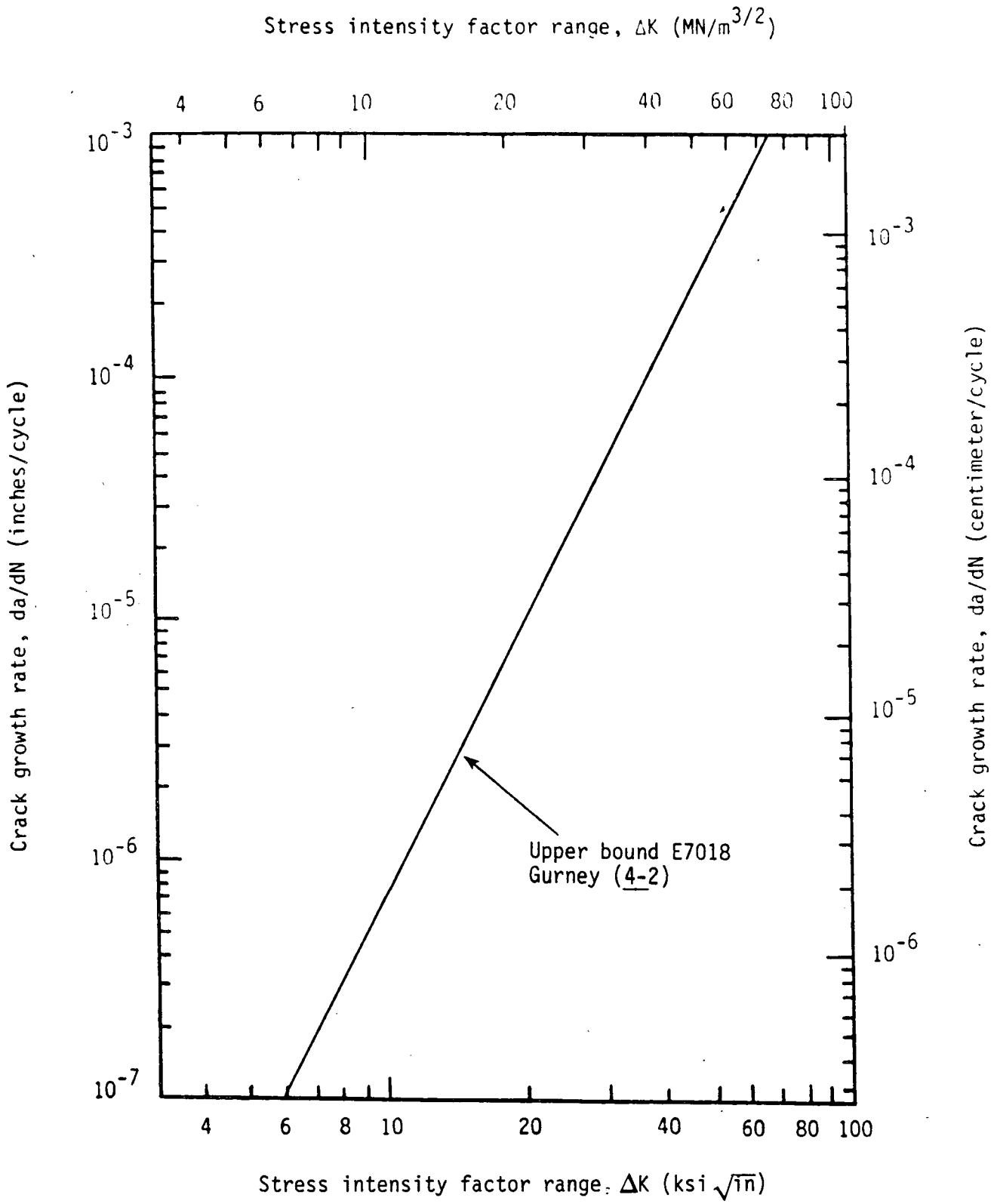

Figure 4-3 - Bounding Crack Growth Line For E7018 Weld Metal.

Section 5

COMPARISON OF DESTRUCTIVE TEST RESULTS WITH LIMIT LOAD PREDICTIONS

INTRODUCTION

Samples of flawed weldments were cut from various HVAC ducts. All samples were examined to establish the dimensions of the lack of penetration, and tensile tests were performed on the samples removed in 1981. Initial tests were performed in 1981 and additional examinations in 1988 ((5-1) and (5-2)). More recently additional confirmatory tensile tests were performed as part of this program. All samples were representative of the ductwork welds but were not taken in a truly random manner. Engineering bias was applied to the samples as follows:

- The locations of the 1988 samples were close to the highest stress regions identified by the stress analysis performed by TVA (3-1).
- The 1990 samples were taken at convenient locations. In all, ten samples were taken and six were tested. Six test results were enough to confirm that the samples were similar to the data generated in 1981 (Figure 5-1).

The sample identification, the lack-of-penetration depth to weld thickness ratio and the resulting ultimate gross section stress (determined using adjoining base material dimensions) are shown in Table 5-1. Table 5-1 also includes a summary of the failure locations. As can be seen in Table 5-1, samples with the smaller lack-of-penetration depths failed in the base metal. These results are typical of welds that contain such imperfections.

The values used in the preliminary analysis (1-1) for lack-of-penetration depths have been checked and found to be conservative with respect to (1) the amount of lack of penetration observed on the sample as scaled from the photograph provided (5-1) and (2) the limit load predictions based on base metal properties.

These destructive test results and associated flaw dimension are plotted on a limit load diagram in Figure 5-1. It is apparent from the trend in the data that for small flaw sizes, the critical applied stress in absence of flaws (i.e., the flow stress) is a value of approximately 70 ksi.

The fracture surfaces of the test samples were also examined in the microscope. In all cases, the fracture surfaces exhibited ductile dimpled appearance confirming that plastic collapse is the relevant failure mode. Typical SEM fracture surfaces are shown in Figure 7-1.

LIMIT LOAD ANALYSIS PREDICTIONS

As discussed in Section 2, limit load provides a bounding method of analysis for structural failure controlled by plastic collapse. In evaluating the test results of flat plate specimens, a separate limit load relationship is used for the plate geometry based on two plasticity theorems (5-3). The first gives rise to lower bound solutions and states that the structure will not fail if the applied forces can be balanced by a redistribution of stress such that the induced stresses do not exceed the flow stress of the material. The second theorem, which is an upper bound theorem, states that the structure will collapse when the rate of external work done by applied forces exceeds the rate of internal plastic work for any collapse mechanism. As the first theorem provides lower bound results, it will be used in the analyses in this report.

Many solutions have been developed to calculate the critical stress for various geometries and loading conditions using the lower bound theorem. Several of these are reported in Ref. (5-3).

A typical duct weldment test specimen is shown in Figure 5-2(a). Figure 5-2(b) was used to model the limit load failure conditions of the duct weldment test samples. The lower bound limit load solutions for this geometry and loading conditions are:

- Pin load edge cracked panel:

$$\sigma_c = \sigma_f \left[\sqrt{1 - 2\left(1 - \frac{a}{t}\right) + 2\left(1 - \frac{a}{t}\right)^2} - \frac{a}{t} \right] \tag{5-1}$$

- Rigidly constrained edge cracked panel loaded in tension

$$\sigma_c = \sigma_f \, (1 - a/t) \tag{5-2}$$

The solution to these equations is shown graphically in Figure 5-3 for a material (i.e., Type E7018 weld metal) with a flow stress of 70 ksi.

The destructive duct weldment test results are also included in this figure. As shown in this figure, the two lower bound limit load solutions and an assumed 70 ksi flow stress accurately bound the test results.

Figure 5-4 shows the same limit load solution for a material (i.e., ASTM A570 Grade A material) with a flow stress of 35 ksi. Clearly the limit load solution (with this assumed 35 ksi flow stress) produces extremely conservative predictions of the failure conditions of these duct weldments. This reflects the degree of conservatism used in the limit load analysis for the duct geometries.

In summary, these comparisons indicate that extension of the lack-of-penetration flaws will be controlled by the properties of the Type E7018 weld metal rather than the adjacent base material. The use of the base metal flow stress will result in very conservative failure predictions.

REFERENCES

5-1 Memo: R. O. Lane (TVA) to C. E. Roberts, "Watts Bar Nuclear Plant - NCR 3761 - Purge Air System - Spiral Welded Pipe" (December 18, 1981).

5-2 Cate, S. N., "Watts Bar Nuclear Plant Weld Throat Measurements of Various HVAC Systems", Tennessee Valley Authority, Report SME-MET-88-075 (June 22, 1988).

5-3 Chell, G. G., "Elastic-Plastic Fracture Mechanics", CERL RD/L/R2007 (January 1980).

APTECH
ENGINEERING SERVICES, INC
© 1990 APTECH

Table 5-1

LACK OF PENETRATION TEST RESULTS

Year	Weld Identification	(a/t_w)	UTS (ksi)	Failure Location
1981	NCR3761-1	0.375	32.4	Weld
	NCR3761-2	0.270	47.4	Weld
	NCR3761-3	0.180	47.2	Weld
	NCR3761-4	0.29	47.8	Weld
	NCR3761-5	0.26	57.0	Base metal/weld
	NCR3761-6	0.18	59.4	Partial base/weld
	NCR3761-7	0.29	48.2	Edge of weld
	NCR3761-8	0.48	46.0	Weld
	NCR3761-9	0.30	38.0	Weld
	NCR3761-10	0.38	42.4	Weld
	NCR3761-11	0.36	46.0	Weld
	NCR3761-12	0.41	44.1	Weld
	NCR3761-13	0.10	60.2	Base metal
1988	47W920-802-0327	0	--	--
	47W920-804-3-0180	0.40	--	--
	47W920-805-2-0062	0.37	--	--
	47W920-804-6-0359	0	--	--
	47W920-804-0262	0	--	--
	47W920-804-5-0322	0.37	--	--
	47W920-805-4-0250	0.28	--	--
	47W915-815-0022	0.36	--	--
	47W920-805-0012	0	--	--
	47W920-802-0005	0	--	--
	47W915-816-0027	0.43	--	--
	47W920-802-0314	0	--	--
	47W915-812-0105	0.05	--	--
	47W920-804-0441	0	--	--
	47W920-805-0362	0.23	--	--
	47W920-802-0552	0	--	--
	47W920-804-0521	0	--	--
1990	804-532	0.36	36.9	Weld
	804-4-214	0.13	59.6	Base metal/edge of weld
	804-4-222	0.31	43.5	Weld
	805-0-343	0.29	46.3	Weld
	805-1-0011	0.19	47.1	Base metal
	805-5-0398	0.27	51.8	Weld

APTECH
ENGINEERING SERVICES, INC.
© 1990 APTECH

LIMIT LOAD ANALYSIS

EDGE CRACKED PANEL – TEST SAMPLES

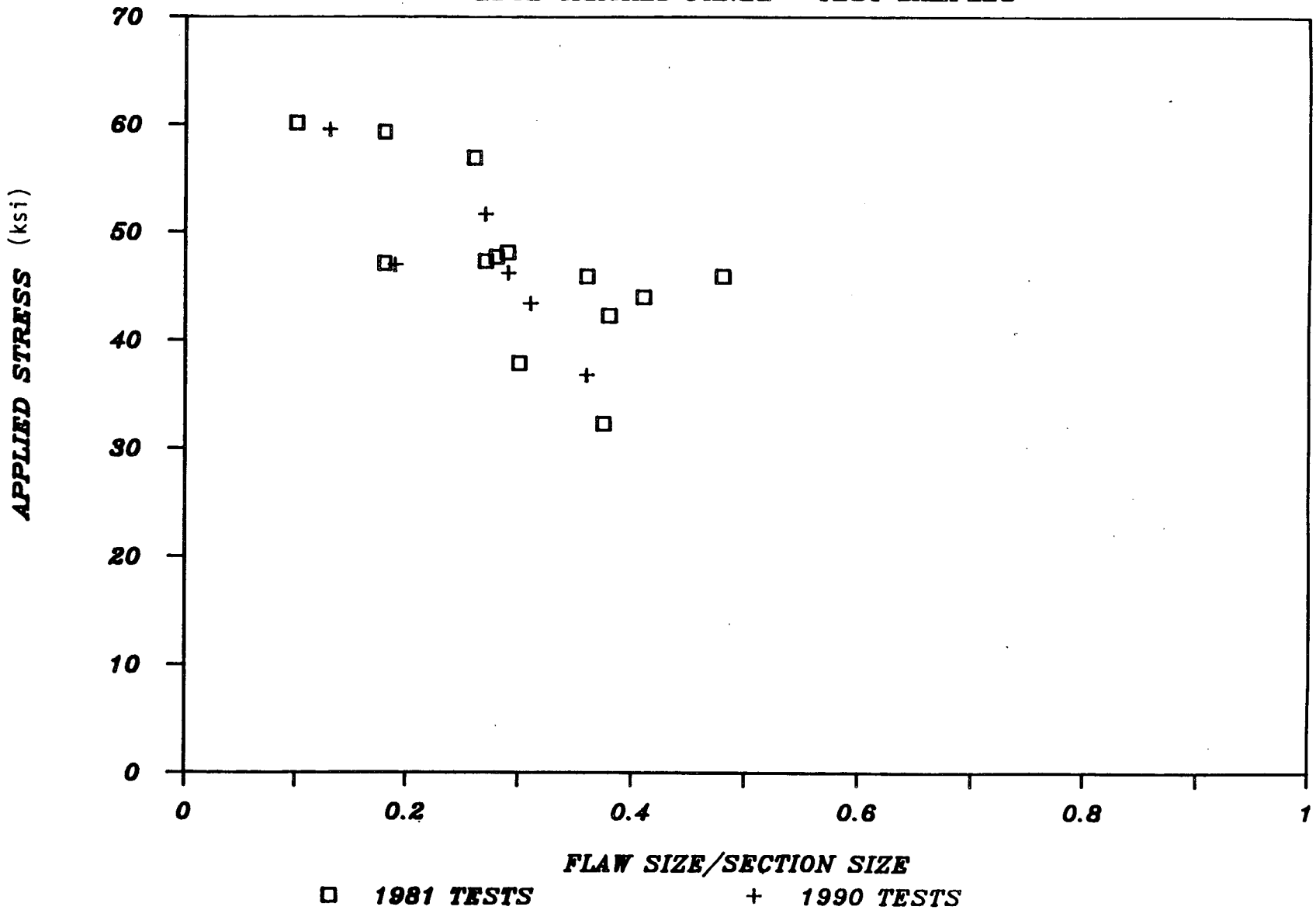

Figure 5-1 - Destructive Test Results Plotted on a Limit Load Diagram.

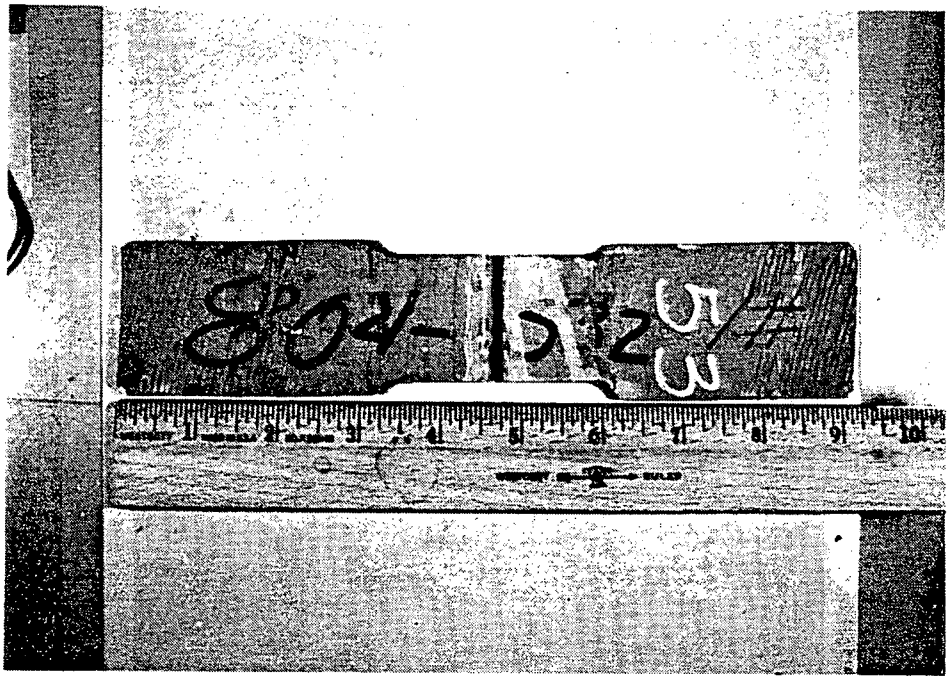

(A) Duct Weldment Test Geometry

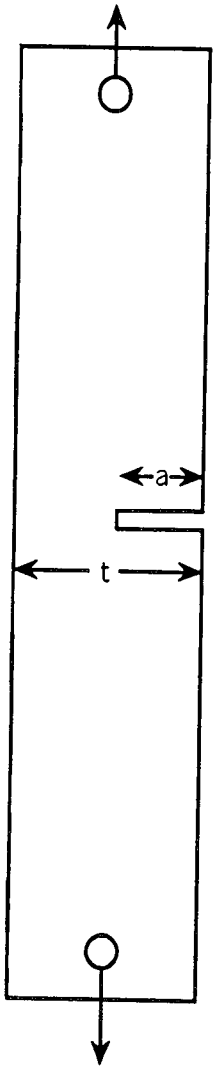

(B) Pin Loaded Edge Cracked Panel

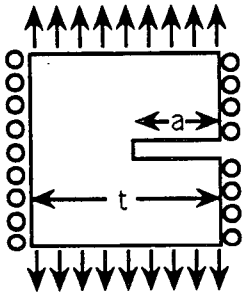

(C) Rigidly Constrained Edge Cracked Panel

Figure 5-2 - Edge Cracked Panel Models Used to Predict the Destructive Test Results.

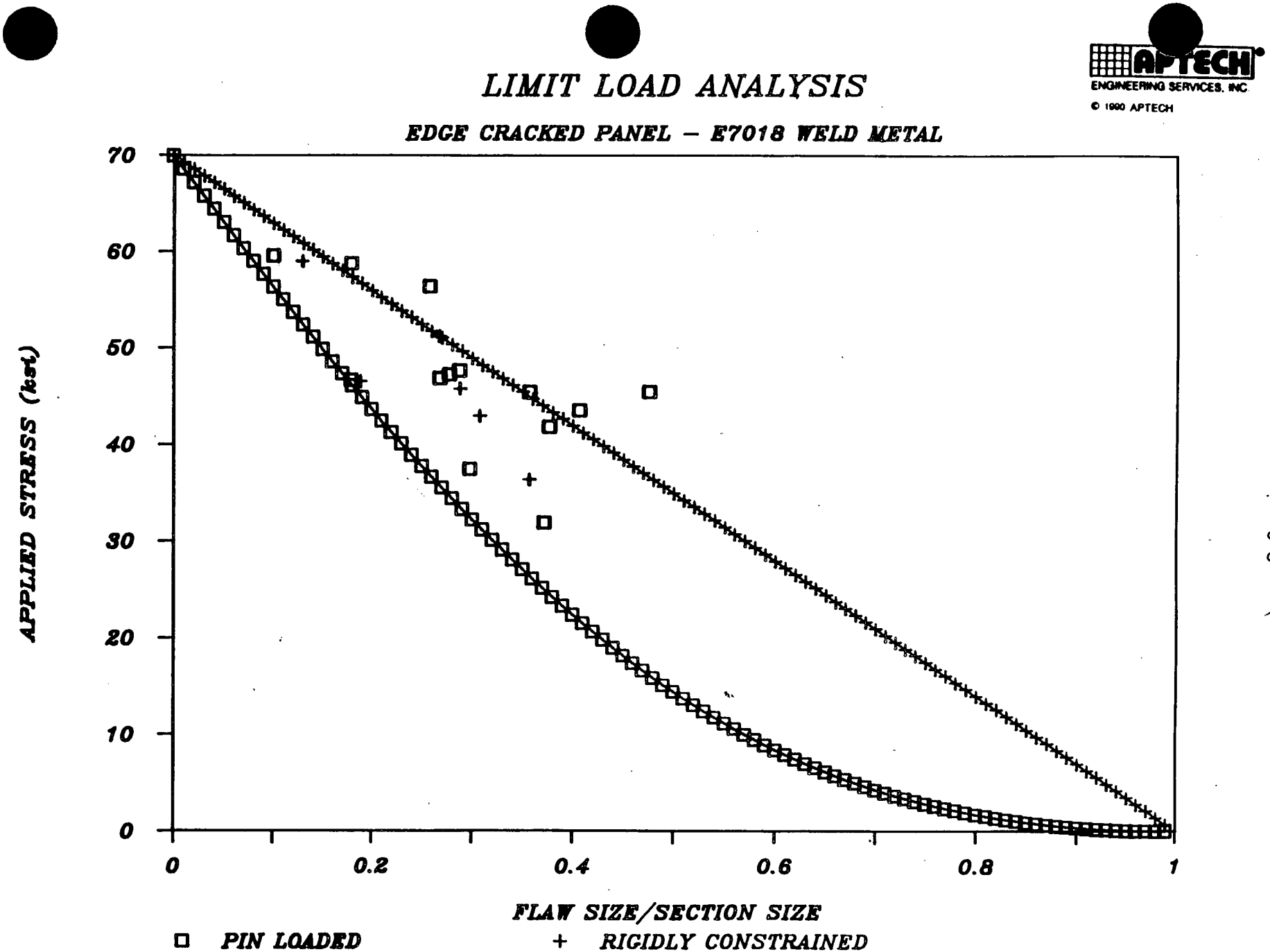

Figure 5-3 - Limit Load Analysis Predictions For an Edge Cracked Plate With Flaws in E7018 Weld Metal.

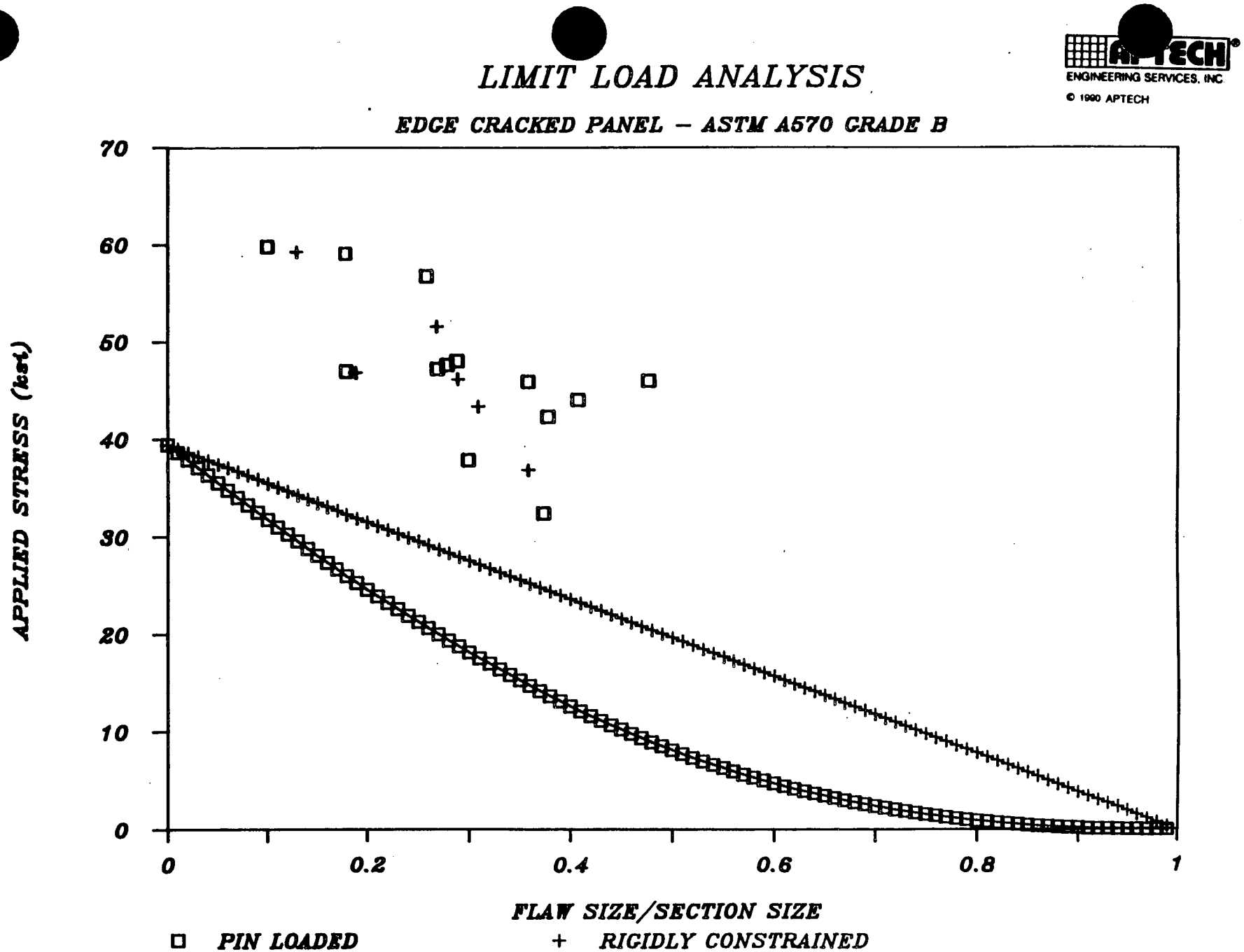

Figure 5-4 - Limit Load Analysis of an Edge Cracked Panel With a Flow Stress of 35 ksi.

Section 6
WORST CASE FLAW SIZES AND APPARENT STRENGTH

INTRODUCTION

A statistical analysis was applied to the key data listed in Tables 5-1 and 6-1. The original data set provided by TVA (6-1) was reviewed at the site by APTECH personnel and TVA. Each entry was checked for relevance to the current issue by reviewing the original walkdown inspection data sheets (6-2). As a result of this review, the data are shown now as that in Table 6-1 (6-3). The scatter in these data is apparent. Because of limited sample size and scatter in the data, a standard "95-95" statistical definition was chosen to establish these "worst case" values. Here, the first "95" refers to a 95% probability of "doing better" than the value quoted. The second "95" refers to the use of a 95% confidence bound. This bound compensates for the lack of an infinite sample size. It limits the chance to 5% that our estimates are too optimistic.

The 95-95 definition of the "worst case" was chosen to be consistent with quality goals in weld quality reverification programs carried out according to the Nuclear Construction Issues Group (NCIG) guidelines (6-4).

FORMULATION OF THE STATISTICS PROBLEM

To obtain conservative bounds on the above data in a convenient way, the following approach was taken. We compute the cumulative probability distribution,

$$F(r) = \text{PROBABILITY}(R \leq r), \qquad (6\text{-}1)$$

for the worst case 1%-10% "tail" of each of three variables of interest. These are:

- R = Uncracked Percentage of Weld Thickness (t_w) = U = 100%(1-a/t_w). Here, a is the measured crack depth.
- R = Acceptable Percentage of Weld Length = APWL. Note that

  APWL = 100%-% of "missing" weld length

- R = Apparent (gross-section) Ultimate Tensile Strength of Cracked Weld Specimens,

  R = AUTS

ASSUMPTIONS

For details about the statistical methods, references, and minor assumptions, refer to Appendix A and the calculation document (A-3). The employed statistical methods and computer program have been checked and verified within the APTECH quality assurance program both in this project and in (A-4) for a different nuclear component application. A list of the major assumptions follows below:

(1) Nonparametric method (i.e., assuming no specific probability distribution function) to estimate both F(x) and its confidence bounds.

(2) Weibull (three-parameter) used initially to fit nonparametric data calculations.

(3) For all three variables, the lower tail region (1% < F(x) < 10%) and its lower 95% confidence bound are the regions of interest. That is, the lower the estimate of any of these variables, the more conservative (pessimistic) are the subsequent limit load and strength analyses.

(4) Accordingly, for purpose of this calculation we have no interest in the upper part of the distribution, F(x) > 50%.

(5) Based on Assumptions 3 and 4, the Weibull fit is used only as a first step. It is adjusted by eye as required to ensure conservative estimates of F(x) at the 95% lower confidence bound.

RESULTS

Figures 6-1 through 6-3 support the following results and conclusions.

(1) Lack-of-penetration depth is less than 53% from the statistical analysis and less than 48% from our worst observation (Figure 6-1).

(2) Missing weld length is less than 17% from the statistical analysis and less than 14% from our worst observation (Figure 6-2).

(3) Apparent ultimate strength of welds with lack of penetration is greater than 28 ksi from the statistical analysis and greater than 32 ksi from our worst observation (Figure 6-3).

REFERENCES

6-1 Tennessee Valley Authority, "Chronology of Events Regarding the HVAC Weldment Evaluation" (June 4, 1990).

6-2 Tennessee Valley Authority, "Walkdown Results Using Procedure WP-26" (June 1988).

6-3 Tennessee Valley Authority, Quality Information Request/Release, Division of Nuclear Engineering, Memo: Geoffrey R. Egan (APTECH) from Roger W. Alley (TVA), Transmission of Percentage of Existing Weld Length, RIMS B26 80 0620 114 (June 20, 1990).

6-4 Nuclear Construction Issues Group, "Sampling Plan For Visual Reinspection of Welds", NCIG-02, Rev. 0 (September 1985).

Table 6-1

PERCENTAGE OF EXISTING WELD LENGTH

Weld Number	Weld Type	Percentage Acceptable (%)
47W910-801-3-0017	Circumferential	86
47W910-801-3-0021	Circumferential	86
47W910-801-3-0023	Circumferential	93
47W910-801-3-0025	Circumferential	98
47W910-801-3-0027	Circumferential	95
47W915-808-0478	Circumferential	90
47W915-805-0185	Circumferential	98
47W915-809-0090	Circumferential	91
47W915-809-0449	Circumferential	92
47W915-809-0595	Circumferential	96
47W915-810-0194	Circumferential	95
47W915-810-0196	Circumferential	95
47W915-810-1-0005	Rectangular	88
47W915-810-1-0006	Rectangular	88
47W915-810-1-0023	Rectangular	88
47W915-810-1-0037	Circumferential	99
47W915-810-1-0038	Circumferential	93
47W915-810-1-0080	Circumferential	95
47W915-810-1-0091	Circumferential	98
47W920-801-0066	Circumferential	99
47W915-805-0061	Circumferential	99.6
47W915-805-0108	Circumferential	98
47W915-805-0114	Circumferential	99
47W930-801-0059	Rectangular	97

APTECH
ENGINEERING SERVICES, INC.
© 1990 APTECH

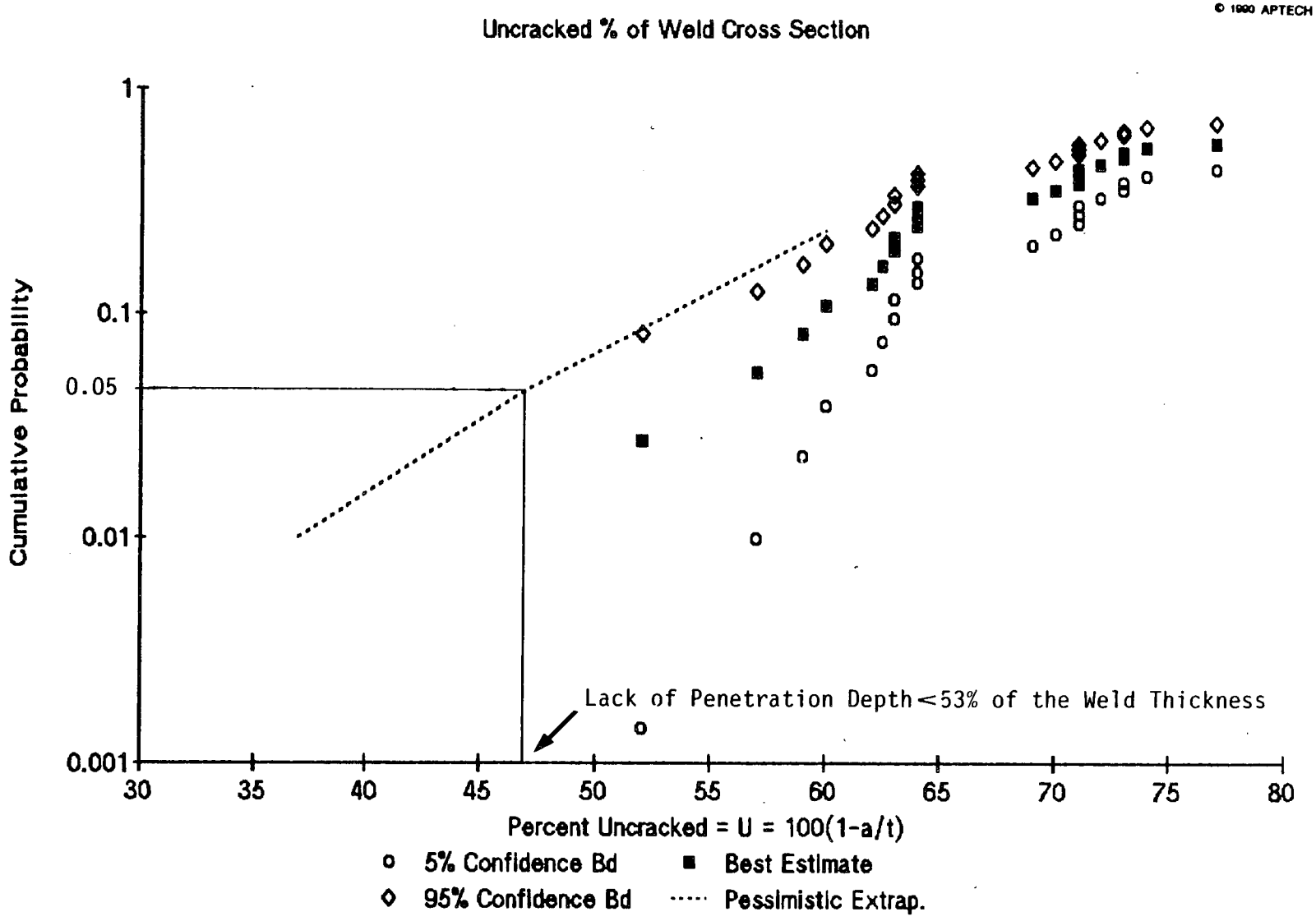

Figure 6-1 - Uncracked Percent of Weld Cross Section.

APTECH
ENGINEERING SERVICES, INC.
© 1990 APTECH

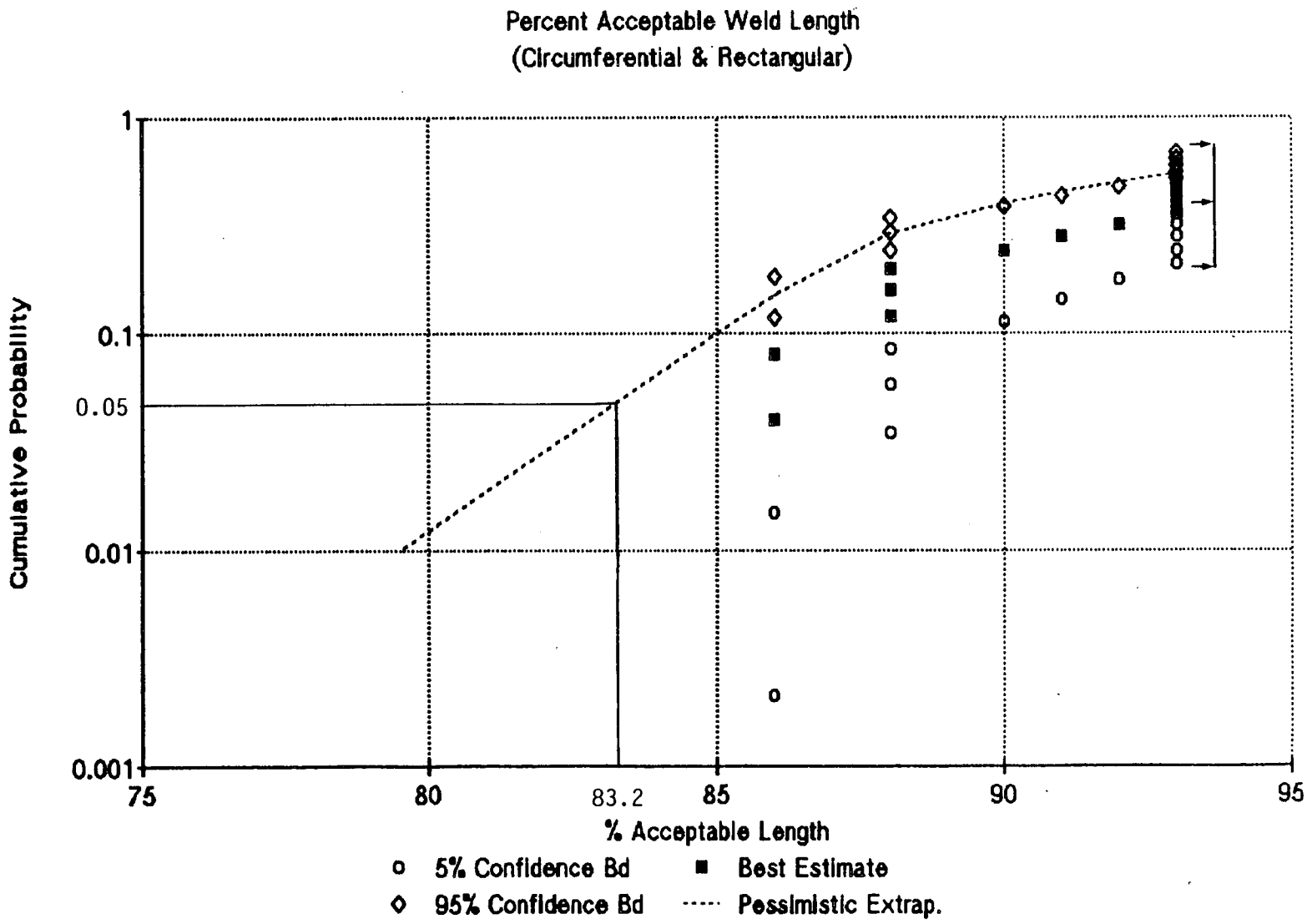

Figure 6-2 - Percent Acceptable Weld Length.

© 1990 APTECH

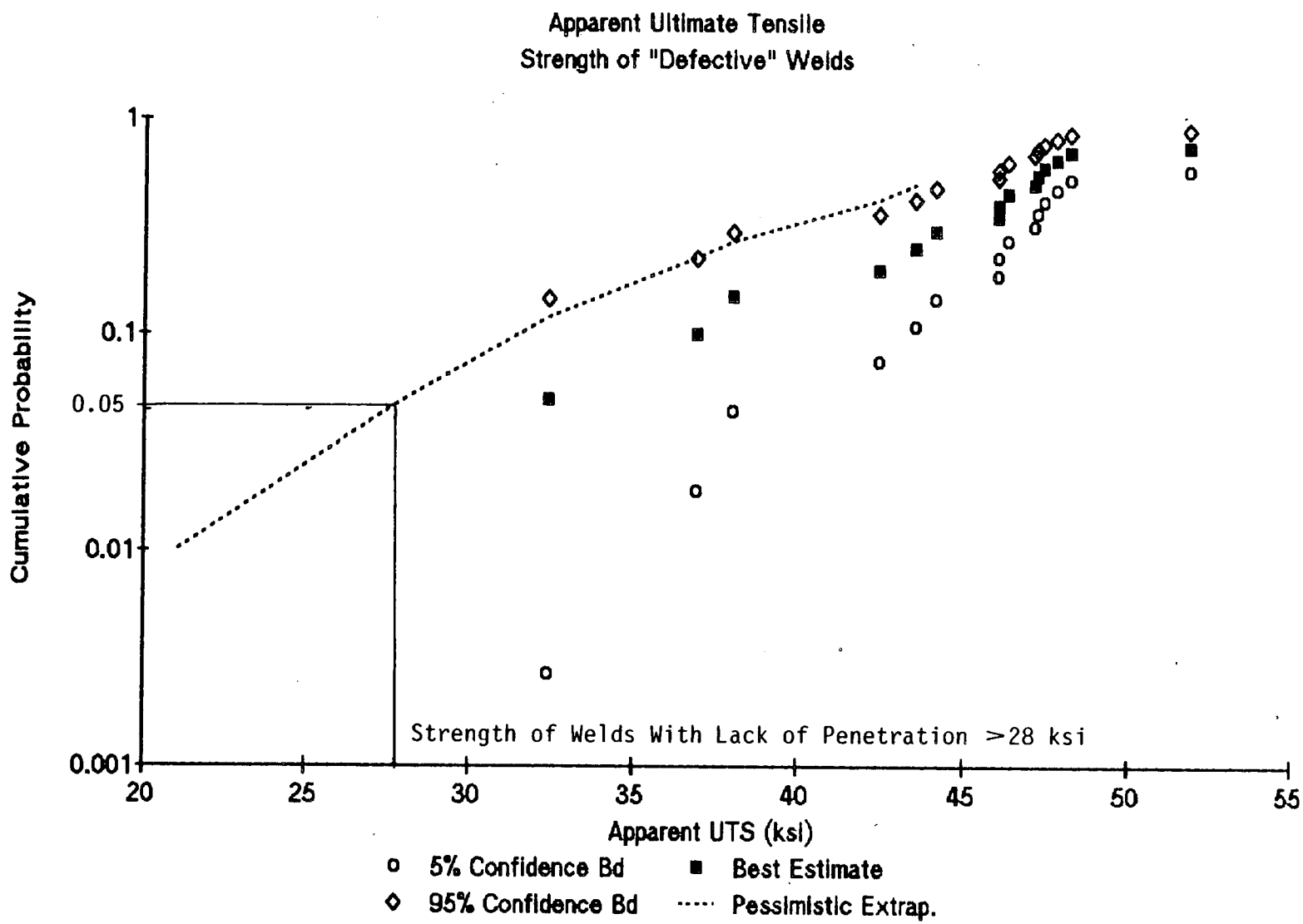

Figure 6-3 - Apparent Ultimate Tensile Strength of "Defective Welds".

Section 7
FITNESS-FOR-SERVICE EVALUATION

INTRODUCTION

Prior sections in this report have established upper-bound stresses to be used in the structural integrity analysis and "worst case, 95-95" weld attributes to be compared to calculated flaw sizes to cause limit load failure. In this section, we develop a fitness-for-service evaluation to determine the significance of the worst case weld attributes.

To confirm that the test samples (and, hence, the ductwork) will exhibit ductile failure, we have examined the fracture surfaces using light microscopy and the scanning electron microscope (SEM). In all cases the failures exhibited ductile dimpled fracture surface appearance. Figure 7-1 shows a typical SEM fracture surface from the samples tested as part of this program.

EVALUATION OF SUBCRITICAL CRACK GROWTH

Using the methods outlined in Section 4, fatigue crack growth has been estimated for the two weld attributes for the following load cycles (7-1):

- Five OBE events at ten cycles per event
- One SSE event at ten cycles per event

The results show that for these low numbers of cycles, the expected flaw growth for the lack of penetration is negligible and for the Sections of weld missing it is small (less than 3% increase in crack size). Such growth does not effect structural integrity.

LIMIT LOAD EVALUATION

A limit load evaluation using the relationships in Code Case N463 (2-1) entitled "Evaluation of Flaws in Ferritic Piping", was performed to assess the integrity of duct weldments which contain either sections of weld missing or lack of penetration.

RESULTS

The results of the analysis are shown in Figure 7-2. The bounding case in Figure 7-2 is for the postaccident sampling piping under normal/upset loading. The stresses for this case are made up of 8.45 ksi secondary stress plus 0.48 ksi upset stress as shown in Table 3-2. This curve also includes the explicit safety factor of 2.77 from the code case.

Also shown in Figure 7-2 are the results of the preliminary analyses and the worst case values for the weld attributes. It can be seen that additional margin exists between the worst case values of the weld attributes and the analysis results.

CONSERVATISMS IN THE ANALYSIS

Throughout the development of the structural integrity analysis, several conservative assumptions and procedures have been used. These are added to the explicit safety margins incorporated in Code Case N463. The explicit margins are the factors of safety of 2.77 for OBE and 1.39 for SSE in Code Case N463. The additional implicit margins are summarized below:

- It is clearly shown by comparing the test data with the predictive method that significant strength is contributed by the weld metal properties. The predictions of structural integrity are based on minimum specified base metal properties. These values are about half of the weld metal values (35 ksi versus 70 ksi).
- The actual material properties will be higher than the minimum specified properties from A570.
- Work hardening effects are limited to a flow stress of the average of the yield and ultimate strengths. Work hardening contributes more to cross section strength.

- Worst case weld crack size attributes have been used in the analysis. These are larger than any observed values. In addition, in the analysis of potential missing weld, we have treated inaccessible welds as if they were missing.

- Worst case stresses for OBE, SSE, and design basis accident (for ductwork supported from the steel containment vessel only) are used in the analysis.

REFERENCES

7-1 Tennessee Valley Authority, Quality Information Request/Release, Division of Nuclear Engineering, Memo: Geoffrey R. Egan (APTECH) from Roger Alley (TVA), Fatigue Consideration For the Number of Seismic Events and the Number of Cycles Per Event, RIMS B26 90 0614 102 (June 14, 1990).

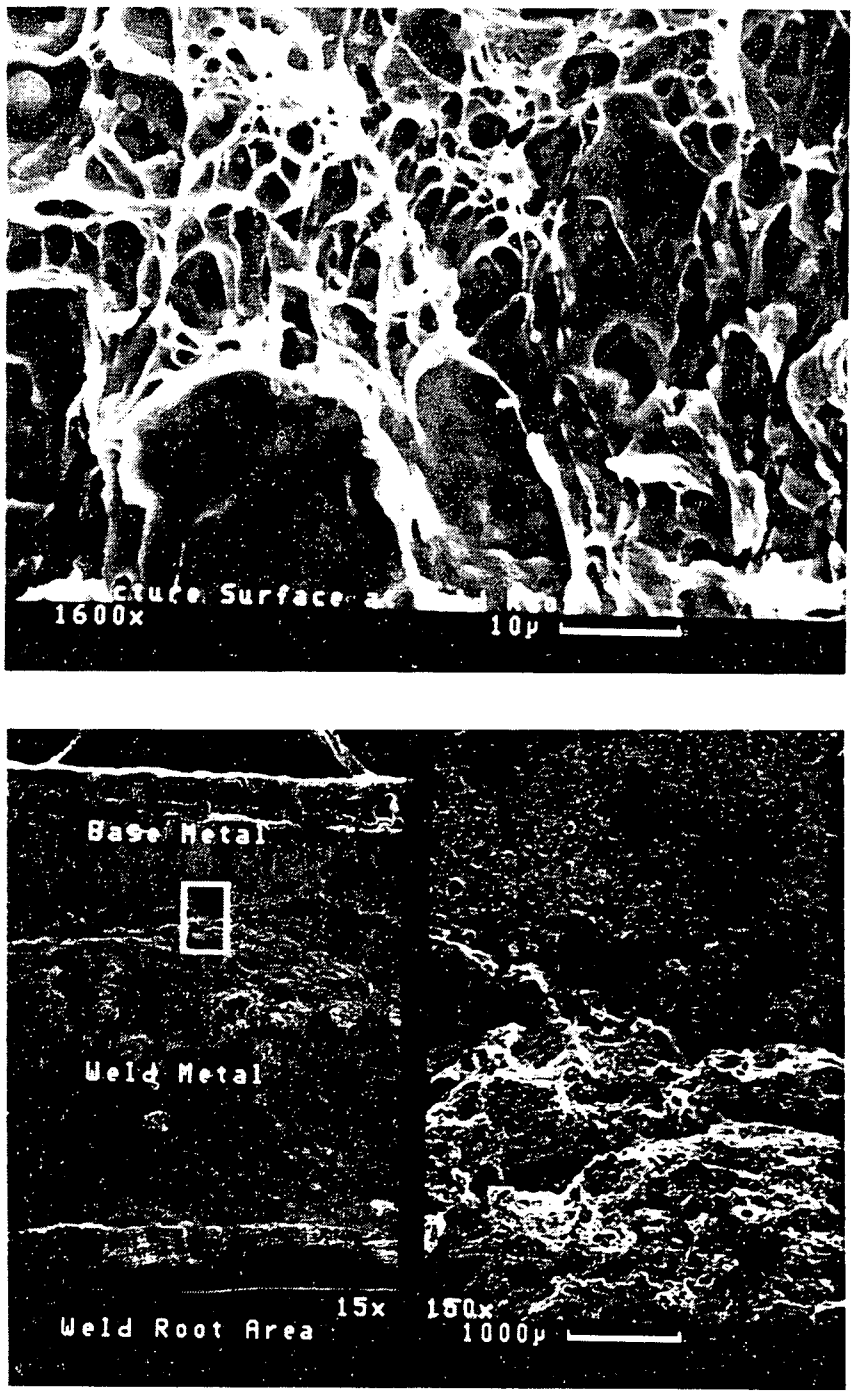

Figure 7-1 - Typical Fracture Surface From Test Sample.

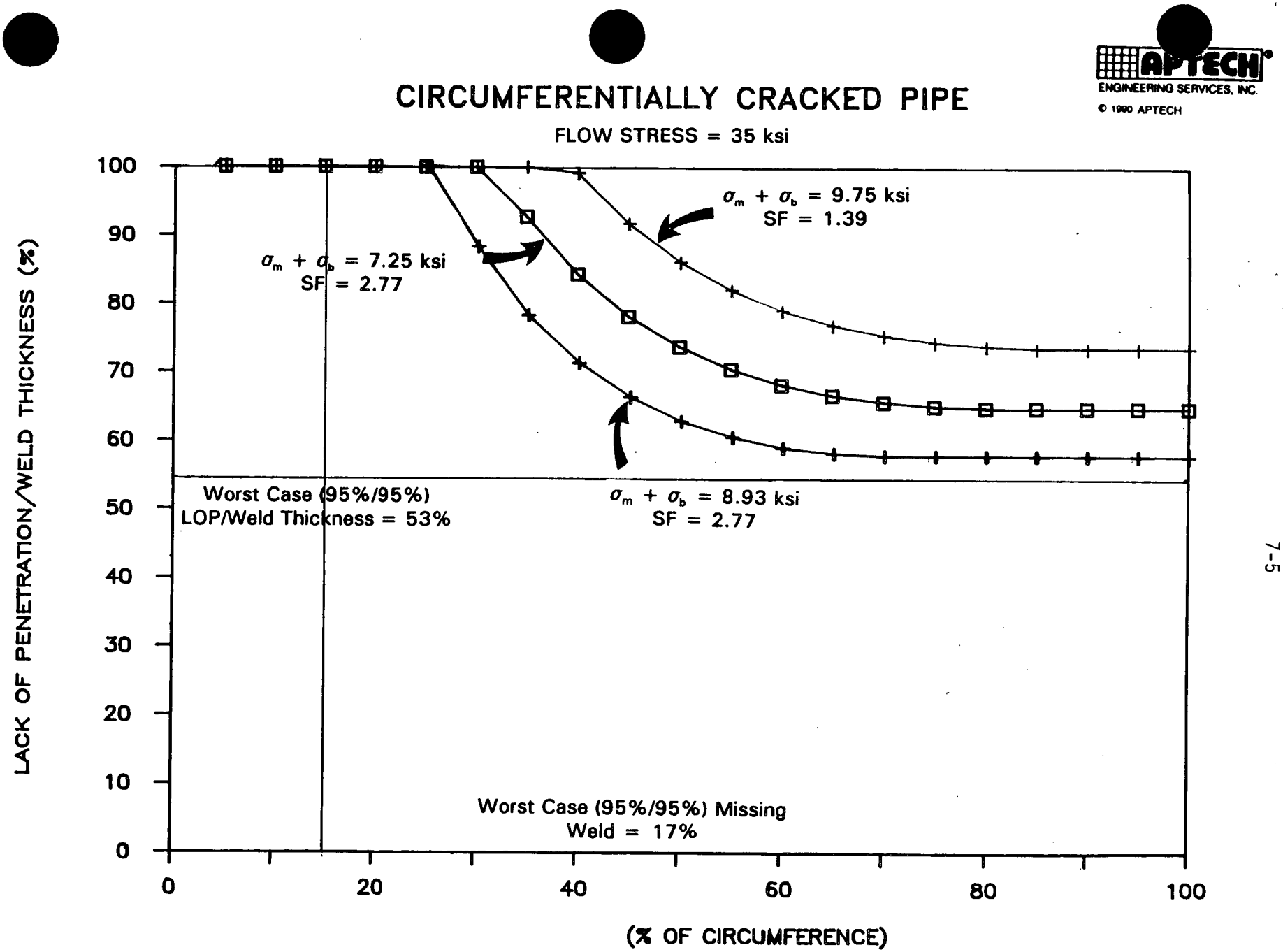

Figure 7-2 - Limit Load Analysis.

Section 8
CONCLUSIONS

- Limit load analysis methods conservatively predict the failure conditions for HVAC ductwork containing potential weld flaws.
- Test results on samples removed from the ductwork confirmed the analysis methods and the strength of the welds.
- Inspection data have been used to establish statistical worst case values for the two weld attributes considered. The results for a "95-95" worst case are 53% for lack of penetration and 17% for potential "missing" weld.
- Even with these conservative worst case estimates of weld crack attributes, significant margins against failure are shown to exist. This finding relied on conservative code analyses and worst case stresses for OBE and SSE.
- Fatigue crack growth is negligible and has no effect on structural integrity.
- The analyses results, the field inspections, and the test data confirm that the HVAC ductwork is suitable for the design loads for which it was intended.

Appendix A

STATISTICAL ANALYSIS METHOD

STATISTICAL ANALYSIS METHOD

A standard nonparametric technique of order statistics is employed to compute upper and lower confidence limits of the cumulative distribution, F(R) of the random variable R. The technique requires no assumed probability distribution model to compute limits and plot data as discrete points. This relieves the analyst from making an arbitrary selection of a model like the normal, log normal, or Weibull distribution.

After executing the nonparametric analysis and plotting all data, the program plots some curves. For guidance only, these curves are three-parameter Weibull distributions used to fit the nonparametric data points. By eye, we used curves in Figures 6-1 through 6-3 more conservative than those plotted by the program.

BEST (POINT) ESTIMATES OF F(R)

Following the recommended graphical procedures of Gumbel (A-1), the mean rank is used to estimate the plotting position (R, F(R)) in a cumulative failure probability plot. Figures 6-1 through 6-3 are such plots. This mean rank is given by:

$$F(R) = i(R)/(N + 1) \qquad (1)$$

where N is the sample size and i is the order number of the value of R. That is, i = 1 is used for the lowest value of R, i = 2 is for the next largest, etc. In other words, the data are ordered by the procedure, so that $R_1 \leq R_2 \leq \ldots \leq R_n$.

The procedure most easily handles "complete" samples for which all the R_i values are known. Also, the procedure handles so-called incomplete samples. These samples contain suspended

data expressed as $R<r$ or $R>r$, not $R=r$. The procedure and software handle any mixture of suspended and complete data.

For suspended data samples, the best-estimate equations for F(R) are:

$$F(R_{i+1}) = F(R_i) + 1/(N_{eff} + 1);\ i = O, n_f \tag{2}$$

where,

$F(R_i)$ denotes the plotting position of the ith of n_f ordered data values for which R is known precisely (i.e., nonsuspended values of R).

$$F(R_o) = O \tag{3}$$

and

$$N_{eff} = \text{Effective number of units with } R>R_i$$

$$N_{eff} = N_t + \sum_{j=1}^{N^-} (R_j - R_i)/(R_{i+1} - R_i)$$

where,

N_t = Number of units for which R is known to be $> R_{i+1}$

N^- = Number of units for which R is known to be $>R_j$, where $R_i \leq R_j \leq R_{i+1}$

Use of the above algorithm is equivalent to assuming a piecewise linear cumulative probability function for observed values of R.

CONFIDENCE BOUNDS $F_r(R)$ OF F(R)

The procedure uses a rigorous nonparametric confidence bound estimation method to handle small sample sizes. This avoids the errors of asymptotically normal distribution confidence levels, which should only be used for large samples. For complete samples in which the value of R of one unit is independent of all other values of R, the exact confidence bounds for the ith order statistic in N are given by the cumulative binomial distribution. Figure 6-4 reproduced from Whittaker and Besuner (A-2) illustrates the relationship between F for the order statistics and the parent distribution (using N rather than i to denote the ith value of R). The specific equation used is given below:

$$\gamma = 1 - \sum_{k=0}^{i-1} \frac{N!}{k!(N-k)!} F_\gamma^k (1 - F_\gamma)^{N-k} \qquad (4)$$

where γ is the specified confidence level and F_γ, defined as

$$F_\gamma = F_\gamma(R_i, i, N)$$

is the desired confidence bound estimate of cumulative R probability. This means that γ is the probability that the true cumulative value F(R) lies in the interval between 0 and F_γ. For all but the simplest situations, the above equation must be solved implicitly through an iterative numerical scheme.

For the case of suspended data, the previous set of equations is used with N_e. Ne is the effective size of the sample rather than the complete sample value N. The parameter N_e is completed from the relationship

$$N_e = (i/F(R_i)) - 1 \qquad (5)$$

for each $[R_i, F(R_i)]$ point plotted.

This procedure accounts for the fact that the fewer the values of R, the less the accuracy in making estimates of R. In general, N_e is not an integer. A linear interpolation is used to estimate the confidence bounds, F_γ for noninteger values.

The specific equation used is given by:

$$F_\gamma(R_l, N_e) = F_\gamma(R_l, NB) + (N_e - NB)(F_\gamma(R_l, NA) - F_\gamma(R_l, NB)) \qquad (6)$$

where N_e lies in the closed interval between the two integers NB and NA = NB + 1.

The above procedure, while complex in nature, has been benchmarked twice against an independent analysis method with fewer capabilities (A-3 through A-5). Reasonable-to-excellent agreement between the two methods was observed.

REFERENCES

A-1 Gumbel, E. J., *Statistics of Extremes*, Columbia University Press, New York (1958).

A-2 Whittaker, I. C., and P. M. Besuner, "A Reliability Analysis Approach to Fatigue Life Variability of Aircraft Structures", Wright-Patterson Air Force Base, AFML-TR-69-65 (April 1969).

A-3 Calculations 3 and 4, APTECH Project AES 90041243-1Q

A-4 Calculation 1166-1Q-6, APTECH Project AES 89121166-1Q

A-5 Cipolla, R. C., J. L. Grover, and P. M. Besuner, "Significance of Over-Drilled Oil Holes on Fatigue Life of the KSV-4-2A Connecting Rod in the Standby Diesel Engines at South Texas Project", APTECH Report AES 89121166-1Q-1 (March 1990) (See Section 3, especially)